~~Mass movements~~ Mass movement mapping ~~inventory map~~ and their impact~~s~~ analysis on the upper Tayyah valley's bridge along Shear escarpment highway, Asir region (Saudi Arabia) using remote sensing data and field investigation

Ahmed M. Youssef [(1,2)], Mohamed Al-Kathery[(2)] and Biswajeet Pradhan[(3)*]

1- Geology Department, Faculty of Science, Sohag University, Egypt

2- Geological Hazards Department, Applied Geology Sector, Saudi Geological Survey, 54141, Jeddah 21514, KSA, Tel. +966-568448782. Email. amyoussef70@yahoo.com

3- Department of Civil Engineering, Geospatial Information Science Research Center (GISRC), Faculty of Engineering, University Putra Malaysia, Tel. +603-89466383; Fax. +603-89466459

*Email. biswajeet24@gmail.com or biswajeet@lycos.com (corresponding author)

Abstract. Escarpment highways, roads and mountainous areas in Saudi Arabia are facing landslides that are frequently occurring from time to time causing considerable damage to these areas. Shear escarpment highway is located in the north of the Abha city (Tayyah valley). It is the most important escarpment highway in the area, where all the light and heavy trucks and vehicle used it as the only corridor that connects the coastal areas in the western part of the Saudi Arabia with the Asir and Najran Regions. More than 10,000 heavy trucks and vehicles use this highway every day. In the upper portion of Tayyah valley of Shear escarpment highway, there are several landslide and erosion potential zones that affect the bridge and the highway between Tunnel 7 and 8. In this study, different types of landslides and erosion problems were considered to access their impacts on the upper Tayyah valley's bridge along Shear escarpment highway

using remote sensing data and field investigation. These landslides and erosion problems have a negative impact on this section of the highway. Landslide and erosional features inventory map was constructed using visual interpretation of the high resolution satellite image and the 3-D image view. The results were aided by a detailed field investigation. This work is not well known in Saudi Arabia and may be considered as the pioneer~~could~~ ~~represent~~ ~~the corner stone for~~work in –landslide hazard analysis. In addition ~~of that~~to the field study, the remote sensing based analysis indicated that the study ~~area have~~areas have different landslides including planar, circular, rockfall, and debris flows. These landslides were evaluated in the current study and some mitigation strategies were considered.

Keywords: Landslides; Inventory map; Erosion; RS; GIS; Mitigation; Asir; Saudi Arabia

1 Introduction

Landslides are one of the natural hazards that cause serious economic and live losses every year all over the world. They hit mountainous areas and highways from time to time due to different triggering factors such as intense rainfall, high groundwater pressures, seismic activity (earthquakes and blasting), rapid snow melting, volcanic activity, and various types of human activities~~ons~~ (Franklin and Senior 1997; Guzzetti et al., 2008a, b; Baum and Godt, 2010; Iverson et al., 2011; Youssef et al., 2012). Cruden and Varnes, 996; Shroder and Bishop, 1998; Regmi et al., 2013a, 2013b, indicated that landslides can be of many types such as: ~~involve~~ flow~~ing~~, slides~~ing~~, toppling, or falling, and complex landslides (a combination of two or more types of movements). In the current research the words “landslide”, “mass movement”, and “slope failure” are used as synonyms. In mountainous areas of the southern Saudi Arabia, there are lots of urban areas, highways, and escarpment roads are prone to different types of landslides such as rockfalls, debris flows, and sliding (planar, wedge, and circular failures) (Youssef et al., 2012, 2014a). Among these landslide problems in Saudi Arabia; the most prominent ones are the Al-Hada debris flow ~~in~~ which occurred in August 2012 (Youssef et al., 2013) and Al-Raith debris flow in March 2013 (Youssef et al., 2014b). Many authors such as Petley (2008) and Van Westen et al. (2006) used different data sources such as field data collection, topographical and geological maps, and satellite images interpretation to prepare landslides inventory map. The work of Brabb (1991) can be considered as one of the pioneer work ~~indicated that landslide~~in landslide -inventory mapping ~~represents the corner stone for several aspects such as documenting the occurrence of landslides phenomena in different areas~~ (Trigila et al., 2010). Similarly, other studies related to landslide analysis are well documented in the literature such as:~~,~~ landslide hazard analysis (Harp et al., 2011a; Guzzetti et al., 2012), landslides susceptibility analysis (Cardinali et al., 2006, van Westen et al., 2006, 2008, Bălteanu et al., 2010, Pradhan and Lee, 2010, Pourghasemi et al., 2012; Xu et al, 2013a; Youssef 2015; Youssef et al., 2013, 2014a, 2014b, 2014c), hazard assessment (Pradhan and Lee, 2007, Xu et al., 2012a, 2012b), distribution of landslides in relation to morphological and geological characteristics (Guzzetti et al., 1996), as well as evaluating the areas that dominated by mass wasting processes (Guzzetti et al., 2008a, b, 2009, Parker et al., 2011). Guzzetti et al. ~~,~~ (2012) indicated that a landslide inventory map portrays the location, numbers and the types of mass movements that have left discernable traces in an area. In the past, before the use of GIS techniques landslides were mapped as points (Plafker et al., 1971, Keefer, 2000). The landslide inventory point map can give some information about the special distribution but not much information about the landslide dimensions and volumes.

There are different methods ~~could be help in~~can be employed for the preparation of ~~preparing~~ landslide inventory maps among them geomorphological field mapping (Brunsden, 1985), visual interpretation of stereoscopic aerial photos (Turnar and Schuster, 1996). However, with the advancement~~ing~~ of computer stereoscopic vision the use of aerial photographs for landslide mapping was expanding (Nichol et al., 2006). Detection of landslides from aerial photographs ~~require~~requires~~d~~ experience training persons and interpretation criteria and methods (Antonini et al., 2002a). In arid and semi-arid areas the morphological appearance of landslides is not concealed by vegetation (De Blasio, 2011). Guzzetti et al., (2015) indicated that landslides can change the landuse / landcover areas and change and modify the visual properties of the land surface. Accordingly, satellite sensors can detect and map these areas easily. Different types of satellite images were used to detect and map landslides such as; L~~l~~andsat and SPOT images (Gagnon, 1975; Huang and Chen, 1991; Vargas, 1992). Generally, t~~T~~errain conditions are mapped and used as an indication for the presence and/or absence of landslides (Lin et al., 2002). Recently, the use of remote sensing technology for mapping and detecting of landslides has increased dramatically. This is due to the availability of high and very high resolution satellite sensors (passive and active types). In general, many authors used optical sensors images to map and detect landslides using visual and analytical methods ~~among them~~ (Cheng et al., 2004; Lee and Lee, 2006; Youssef et al., 2009; Martha et al., 2010; Fiorucci et al., 2011; Parker et al., 2011; Youssef et al., 2013, 2014a, 2014b). Other authors used Synthetic Aperture Radar (SAR) to detect, map, and monitor landslides ~~among them~~ (Ferretti et al., 2000; Hooper et al., 2004, 2007; Guzzetti et al., 2009; Lauknes et al., 2010).

Several attempts ~~were used~~have been made to map and detect landslides including the interpretation and analysis of high and very high resolution satellite images, digital elevation model (DEM), and 3D-image view. Pan sharpened images ~~were~~ have been applied for landslide mapping (Gao and Maroa, 2010; Fiorucci et al., 2011; Marcelino et al., 2009) whereas Li~~I~~DAR DEM was used by Van Den Eeckhaut et al., 2007; Hanebery et al., 2009). In a recent paper, Harp et al. (2011a) indicated that DEM is an essential in landslide mapping. However, Xu (2014) indicated that DEM is less important because landslides can be detected based on ridges and drainages on remote sensing images. He also concluded that using DEM ~~for prepare~~ the 3D-image view of areas can be very powerful tool for detecting and mapping of landslides. In addition, very high resolution satellite images can be combined with high resolution DEM to provide a 3-D image view of the area and by visual interpretation landslides can be mapped and detected (Nichol et al., 2006; Bajracharya and Bajracharya, 2008; Youssef et al., 2009, 20013). High and very high satellite images represent a good and an accurate alternative data to the aerial photographs and can be used to detect and map landslides (Casagli et al., 2005; Marcellino et al., 2009; Youssef et al., 2013, 2014a, 2014b).~~-~~ Recently, Gao and Maroa (2010); Fiorucci et al. (2011) compared the results of ~~using~~ high resolution satellite images and aerial photographs ~~for the~~of similar resolution ~~and~~ of the same area to detect and map landslides. Their results showed that satellite images can provide similar and complementary landslide information. Xu (2014) indicated that analysis of the image texture and tone can differentiate and map landslide areas from the surroundings. However, this needs ~~the used images must be~~ continuous images ~~and cover~~ covering the entire area with~~,~~ resolution ~~has to be~~between high to very high, and free of clouds. Using the high-resolution satellite images, historical landslides could be observed as breaks in the highly vegetated area, bare soil, or geomorphological features, such as head and side scarps, flow tracks, and soil and debris deposits below a scar (De la Ville et al., 2002, Youssef et al., 2009).

Slope failures can be classified into two groups; first group is depending on the geometrical and mechanical nature of the discontinuities and the conditions of the rock masses which include Circular, Planar, Wedge, and Toppling failures (Farrokhnia et al., 2010; Regmi et al., 2014; Youssef et al., 2012; 2014b). The second group is rock failure by rockfalls and debris flows mechanism which cannot be analyzed using limiting equilibrium analysis. Many authors studied the debris flows, their types, and mechanisms~~,~~ (~~among them,~~ Hungr, et al., 2001; Johnson, 1984; Pierson and Costa, 1987; Youssef et al., 2012, 2014b). Due to the high density and mobility of debris flows, they represent a serious hazard, which impose serious problems for people, properties, vehicles, and infrastructure in mountainous regions. Landslide types such as structural control, rockfalls, and debris flow need ~~a mitigation strategies~~mitigation strategies that may be required to minimize their risks which have been applied in many ~~research~~ areas (Frenez et al., 2004; Maerz et al., 2014; Rickenmann, 1999; Rimbock and Strobl, 2002; Youssef et al., 2012, 2014b).

In t~~T~~he current study, one of the main purposes of this paper is to emphasize the necessity to establish landslide and erosion features inventories, which would make the future landslide inventory maps more objective and consistent. This study deals with the evaluation, mapping, and determination of the characteristics of the different types of problems related to landslides and erosion features and their impacts on the bridge and highway section along the upper portion of Shear escarpment highway (Tayyah valley), which is located between tunnel 7 and tunnel 8. This area is a landslide prone area due to the adverse geological formation, structural features, steep slopes, drainage gullies and rills, highly dissected topography, and rainfall impacts. In this research, field investigation was done to cluster different slope failures that have a major impacts on the highway areas and bridge were studied in detail. In addition, different techniques and tools were used to prepare landslide inventory map for the study area using high-resolution satellite image and high resolution 3D-image view. The principles and techniques used include that all landslides should be mapped as long as they can be recognized from field surveys and images and both the boundary and source area position of landslides should be mapped. We consider methods and techniques for mapping the surface characteristics of landslides of different types, with some geometry and characteristics of slope failures. Most landslides in the study area were detected ~~according to the use of~~based on the field investigation data and interpretation of high resolution satellite image and 3D-image view. According to the use of the high resolution data the smallest scale of landslides was few meters length.

2 Study area

Shear escarpment highway is located in the Asir region, Saudi Arabia (Fig. 1a). It represents a part of Abha Highland (which is related to Arabian shield). It descends from the top of the escarpment (highly rigged mountains) near the Abha City down to the Mahail Asir then to the coastal zone of the western Saudi Arabia (Fig 1b). It connects the Red Sea coastal areas (western region of the Saudi Arabia) with the Asir and Najran regions. This escarpment road is one of the first roads in the area constructed through extremely rugged mountainous terrain about 32 years ago. It is an important escarpment highway, as it offers access to the private vehicles, light-duty trucks, and the only escarpment highway for the heavy duty trucks. The Shear escarpment highway is about 16 km long, measured from the top of the escarpment (2200 m above sea level (asl)) from east to the Mahail Asir city (approximately 700 m asl). The highway is characterized by the presence of about 11 tunnels and many vertical and horizontal curvatures as well as some bridges. The current study is carried out to deal with the bridge and the highway section (with a total length of 2150 m) located between tunnels 7 (at elevation of 1888 m) and 8 (at elevation of 2004 m) at the upper reach of Tayyah valley (Fig. 1b). The area is located on a small wadi that meets at a right angle with the main wadi of Tayyah (Fig. 1b). The small wadi that includes the study area is surrounded by high mountains with steep slopes. It appears as a deep and narrow gorge. This tributary (small wadi) flows with great force in steep and narrow channels often resulting in excessive toe erosion. The area is commonly prone to landslide activities (sliding, rockfalls, and debris flows) and erosion features due to running water through different gullies and rills. There are numbers of active landslides which are badly affecting the highway and bridge section and are the potential sites to cause disaster in the event of a major rainfall or earthquake.

Fig. 1. About here

3 Methodology

In general practice, landslide hazard of an area is assessed by carrying out intensive field investigation, remote sensing data analysis, interpretation of geological and topographical data. This is usually accomplished by the analysis of several maps and landslide distribution of the area to classify them into various types. In the present work, assessment of landslide and erosion problems have been carried out with the help of different data types (Fig. 2). Lithological, morphological, hydrological, and structural characteristics of the study area might have influenced the distribution of landslides and erosional features. The geological and structural data were mapped according to the Abha quadrangle geological map (GM-75, 1: 250,000-scale). These geological and structural data were verified in the field. Many structural data were measured including joint planes and faults. All landslides, in the study area were identified and mapped using high resolution satellite image (QuickBirds 0.61 m spatial resolution from the year

2012), and 3D-image view and verified using intensive field investigation. The high resolution satellite image (QuickBird 0.61 m resolution) was overlaid~~y~~ on the high resolution DEM ~~was done~~ to prepare a 3D-image view (0.61 m resolution) ~~that will help in~~in which was sued to detect~~ing~~ and map landslides and erosional features in precise and accurate way. The high resolution DEM was ~~created~~ constructed from the interpolation of a digital topographic map 1:10,000 scale for the study area. These data were used in retrieving information related to topography, existing landslides, debris accumulation and other relevant features in relation to slope instability and erosion features. The satellite image was registered with reference to the topographic map of the study area by taking input ground control points from the image and reference points from the map. All the images were in UTM coordinate system, Zone 38, and WGS84 datum. Besides mapping the different types of landslides, rock mass rating (RMR) for different rock zones in the study area was identified to determine the quality of these rocks and to classify the study area into different zones. For that purpose, d~~D~~ifferent rock samples were collected from the ~~different~~ each landslide zones in order to apply rock shear test to determine the friction angle for rock plane sliding. Potential for planar failures was carried out using Dips 5 program (RocScience, 1999). Other types of failures such as circular, rockfalls, and debris flows were highlighted and mapped in the field. In addition, gullies~~,~~ that dissect the study area~~,~~ were mapped and different morphometric parameters were determined using watershed modeling system (WMS8.1). Different features of landslides and erosions were mapped using rigorous field investigation ~~and~~ as well as from the 3D-high resolution satellite image view for the study area. The remote sensing based analysis, field, and laboratory studies were coupled together to get the comprehensive view of the different types of landslide and erosion features that impose a high impact on the study area.

Fig. 2. About here

4 Geomorphology, geological/structural setting and climatic characteristics

Geomorphologically, the study area is located at the upper portion of Tayyah valley. The escarpment itself is the result of erosional retreat of uplifted Precambrian rocks that were elevated concurrent with initiation of rifting in the Red Sea during the late Paleogene era. The escarpment runs in different direction such as east – west and north – south. Whereas, the study area has a curvature shape (Fig. 1b).

Geologically; the study area is mainly located in the Bahah group within the Tayyah belt (Abha quadrangle GM-75; Greenwood, 1985) (Fig. 3a). The Bahah group is a major component in the western part of the Tayyah belt. It consists of a fault bounded blocks including abundant volcanic greywacke, local boulder conglomerate, carbonaceous shale, slate, chert, bedded tuff, and interbeds of volcanic flow rock. In the study area there are abundant of greywacke and slate. Greywacke is characterized by massive to thin bedded in form and has sedimentary structures including grading, cross bedding, and lamina bedding. Massive greywacke forms thick beds from 1 – 3 m and interlayered with fine grained and laminated bedded of slate which are strongly metamorphosed to green schist facies. The Bahah group rocks in the Tayyah belt are weakly to moderately cleavage where as they are highly cleaved near faults. They are characterized by the presence of one cleavage (schistosity) which has steep dips toward east or west. Some intrusive rocks including granodiorite and granite were encountered in the Tayyah belt. Near the intrusive contact amphibolite grade metamorphic rocks were encountered. Other rock units are encountered in the surrounding areas include, alluvium and gravel, basalt and andesite, biotite monzogranite, biotite-quartizite-plagioclaae granofels, hornblende-biotite tonalite and granodiorite, Jeddah and Bahah groups, and Muscovite –biotite tonalite and granodiorite.

The area is traversed by many faults where many shear zones are formed. These tectonic features are responsible for crushing and shearing of the rocks in the region. Different types of structures such as faults, folds and linear structures are encountered in the study area and its surroundings according to geological map (Abha quadrangle GM-75) (Greewood, 1985) (Fig. 3a). The geological map was verified by field investigation. Along the main curvature of the study area there is a major fault that cut through the rocks (Fig. 3a). The materials along the fault zone are highly crashed and weathered whereas the rocks become highly sheared and jointed as the distance increased (Greenwood, 1985) (Fig. 3b, c).

Climatically, Saudi Arabia is classified as an Arid to Semi-Arid region according to the "World Map of Kopper-Geiger Climate Classification" (Peel et. al., 2007). The study area is characterized by mild summers and cold winters. According to the analysis of rainfall station (A130, operated by the Ministry of Water and Electricity (MOWE) which is located in the southwest of the study area by about 20 km. Rainfall is typically occurs in intense thunderstorms from March to May. The average monthly precipitations were 29.5, 46.5, and 64 mm for March, April, and May respectively. The average annual precipitation is reported as about 273 mm/year, with a maximum rainfall of 1043 mm occurring in 1997. The maximum precipitation happened in a day was 180 mm in 2004.

Fig. 3. About here

5 Results and Discussion

5.1 Detailed field investigation

Existing and potential landslide areas were identified through detailed field investigation along the upper portion of the escarpment highway and bridge section of Tayyah valley (between tunnel 7 and Tunnel 8) (Figs. 4 and 5). This includes determination of~~e~~ ~~the~~ RMR characteristics of the study area as well the different types of landslides. The rock characteristics along the study area were classified into three zones (Fig. 4) according to the application of the rock mass rating system. In the current study, the RMR system was used in the analysis of the rock masses along the study area. The system first designed to analyze the rock conditions in tunnels but it was modified later to analyze slopes and foundations. The RMR system was applied on the 10 stations along the study area (Fig. 6). Its value was computed, according to Bieniawski (1979), by adding rating values for five parameters including, (1) strength of intact rock, (2) RQD (measured or estimated), (3) spacing of discontinuities, (4) condition of discontinuities, and (5) water inflow through discontinuities (estimated in the worst possible conditions). The RMR value ranges between 0 and 100 has been calculated using VP EXPERT program developed by Ware Inc (1985-1988). Analysis results of rock mass rating RMR for all stations are shown in Table 1. The results indicate that there are three zones in the study area: 1) High foliated rocks are characterized by completely schistose and the RMR values range from 19 to 35 which is from poor to very poor rocks. The strength of these rocks are low to very low (Fig. 4, Table 1). 2) Fault zone is characterized by highly sheared rocks and mostly crashed, main debris flows are formed in this zone due to the presence of crashed materials and colluvial materials. The physical characteristics of these materials are composed of some boulders up to 0.5 m in diameter embedded in gravelly and fine sandy materials. The RMR values range from 16 to 19 which is very poor rocks (Fig. 4, Table 1). 3) Moderately jointed rocks which are characterized by semi massive rocks, sometimes low to moderately strong and characterized by the presence of planar and rockfalls types of failure; they are intruded by some felsic dykes. The RMR values range from 65 to 74 which is good (Fig. 4, Table 1).

Fig. 4. About here

Table 1. About here

Landslides in the study area were mapped, identified, and classified into rock slides (planar and circular failures), rockfalls, and debris flows. The planar failure type is predominantly along discontinuities. The rockfalls and sliding failures (planar failure) are mainly located in zone 1 and ~~&~~3 (Fig. 5a, b, c). In the curent study three sites ~~impose~~ have encountered planar failures from time to time and they were thoroughly examined. These failures are located in Bahah group which is characterized by weakly to moderately cleavage and highly cleaved near fault zone. Sometimes they are characterized by the presence of main joint set (schistosity) which has steep slope toward the bridge section as in site 3. Some intrusive and volcanic dykes were encountered in the Tayyah belt. These gives large planar failures along the main joint set that dips toward the bridge section as shown in sites 1 and 2. Data collected from these three sites, including the main joint set for each site that dip toward the bridge section, were plotted on stereonets (Fig. 6). Sites 1 and 2 are located in moderately jointed zone and their main joint sets are characterized by a dip directions ranges from 7^{o} to 17^{o} and dip angle from 48^{o} to 59^{o} (Table 2, Fig. 7). Field investigations, for these two sites indicate that both are ~~examined~~ large planar failures. By comparing the strike of the bridge section and these two locations indicated that they are nearly parrallel to each other. In addition, the site 3 is located in higly foliated rocks showing a shestosity texture and the main joint set has a dip direction of 5^{o} and dip angle of 80^{o} which is parallel to strike of the bridge section. The dip/dip direction measurements ~~that~~ which was collected from these three sites were plotted on stereonets using Dips 5 software (RocScience, 1999). Stereographic analysis allowed~~s~~ ~~investigators~~ us to visualize and measure discontinuities in three-dimensions by projecting~~on~~ discontinuity planes through a sphere and observing the trace of the line of intersection of the plane and sphere (Fig. 7). A structural control stability analysis utilizing the Markland Test Plot method, was used to assess the potential for planar sliding along the identified discontinuities. Markland test plots show the discontinuities in relation to potential planar sliding surfaces on a lower hemisphere stereonet projection. The slope face is shown as a marked great circle and the measured friction angle is represented by an interior circle. Based on discontinuity roughness and other properties of the rock, friction angles of the collected samples from the three sites have been meaured using different techniques including 1) Rock data analysis of the field rock mass characteristics; and, 2) Rock shear box for the samples along the critical joints in these sites. The lowest friction angle and dip direction of the joints and rock cut were used to determine the potential planar failure. If discontinuity dip vectors plot within the shaded areas of the test plot, failure along the discontinuity is kinematically possible. Table 2 shows the different characteristics of each site and Fig. 10 shows the stereonet presentations of the main discontinuity data collected from the rock cut stations above the bridge section of the study area. In the current study lowest measured friction angle of 35º, 40º, and 30º was used for these three sites respectively (based on the shear strength and rockdatat analysis) Table 2. The dip vectors of these three main joints sets occur within the crescent shaped shaded area, in addition the strike of these main joints have an angle less than 20º from the strike of the rock cut face and so planar failure for these main joints are potential.

Fig. 5. About here

Fig. 6. About here

Table 2. About here

Fig. 7. About here

In zone 2 (fault zone), field investigations showed that the area is highly affected by fault and most of the rock in the area is highly jointed, weathered, and crashed. These highly crashed rocks are mixed together and with the colluvium soils that located with different sizes (Fig. 5d, k). Generally, circular failures have no structural pattern and the failure surface is free to find the line of least resistance through the slope and the failure geometry is circular (Hoek and Bray, 1981; ~~and . (~~Hoek ,1982). Many circular failures were detected in the study area (zone 2) and some of them are clearely appeared in Fig. 5d, e. Whereas other circular failures are new where some tension cracks begin to be appeared at the upper portion of the bench located above the bridge level (Fig. 5f, g). Sometimes complex circular failures are detected in which multiple failure modes, many tension cracks, and subsidence are located along the highly sheared and colluvial materials above the bridge level.

Rockfalls are occured due to a combination of different factors and not related to the structures (joint planes). In most of the rock cuts and slopes, rockfalls are difficult to analyze. Badger and Lowell (1992) mentioned that large number of accidents and about half dozen fatalities were related to rockfalls in the last 30 years. In the study area, most of rockfalls are related to the effect of undercutting of the week materials or due to sliding effect and leave other blocks hanging over, others related to erosional effect of rainfall especially in debris and colluvium materials where the weake materials eroded and leaving large blocks without any support (Fig. 5h, i). With the effect of gravety, rainfall, and vibration due to heavy trucks, these overhaning materials will fall down.

In the study area, the debris flows are mostly confined along natural drainage lines as well as along the fault zone. Debris flows are occurring along the gullies with an average slopes that vary from 13.2^{o} for channel (1) to 32.2^{o} for channel (7) (Figs. 5a, j, k & 9). Most of the debris flows occur along the gullies where loose overburden materials on such slopes, when saturated during rains causes debris flows. This happened very often and these debris flows have an erosion effect along the gullies and between the bridge piles. Where most of weak materials, highly jointed rocks, and colluvial soils erode and moved downwards with running water. The debris flows from these gullies extend below the road and bridge level to the main wadi. Figure 5a, j, k show some examples of debris flow channels and erosion features along the gullies in the study area.

Other type of threatening problem that is related to the erosional effect of the running water through the drainage channels (gullies) that cut through the mountain and run under the bridge and through culverts. There are many drainage channels (gullies) ~~that~~ were found in the study area that impose erosion impact under and between the bridge piles and under the culverts (Fig. 5a, j, l, m). The erosional and debris flows could be a problem in the future and will pose threat to the stability of the bridge and cause damages to vehicles and disrupts traffic.

5.2 Erosion problems under and between the bridge piles

Many authors focused their studies on rill and inter-rill erosion (Poesen and Hooke, 1997). Others focused on gullies erosions and they indicated that these gullies represent the main sediment source in Mediterranean environments (Casali et al., 1999; Poesen et al., 2002, 2003; Valcarcel et al., 2003). The erosion processes in the study area have a severe effect in the areas between bridge piles and the area along the drainage channels (gullies). In the current study, detailed drainage network were drawn from the high resolution satellite image and filed investigations and were compared with the networks that extracted from SRTM 90 m and Digital elevation model of 5 m resolution (created from topographic map of 1, 10,000)) using watershed modeling system (WMS 8.1) (Fig. 8). Different types of morphometric parameters were determined for each gully to determine its activity ~~in~~ on erosion effect (Table 3). Existing and potential erosion areas were identified through field investigation along the study area and by using high resolution image. The erosion materials can cause the debris flow to occur after the gradual increase in discharge. Width of the existing gullies ranges from 6 to 15m whereas the depth of erosion~~s~~ was determined to be from 2 to 5 m (Table 3). Field investigation indicated that most of the gullies have~~are~~ cut through foliated rocks (zone 1) which includes channels 6, 7, 8, 9, and 10, and the fault zone (zone 2) which includes channels 2, 3, 4, and 5. However, few gullies are located in moderately jointed rocks (zone 3) which include channel 1. In the study area most of rocks here are highly foliated (metamorphic), sometimes intruded by different dykes (of acidic igneous rocks). These rocks are overlaid by loose residual soils and slope wash. After the rainfall and with continuities of debris flow, the loose soil cover (debris materials and crashed rocks along the fault zone) are moved away and bare rocks are now exposed on the side walls and at the bottom of the gullies (Fig.5a, j, k, l, m). At the surface of the rocks, and between the bridges piles there are scouring effect (erosions). These debris coming from these areas moved with water toward the main wadi course. Data analysis and field investigation indicated that there are three factors that play a major influence in the erosion processes and which are claimed to be the most important causes of channel erosion. These factors include high runoff due to intense rainfall, weak materials that is located along the gullies, and the steepening slope of these gullies (Table 3).

Fig. 8. About here

Table 3. About here

5.3 Landslide and erosion inventory map

In the current work, the computer screen based visual interpretation of high resolution satellite image (QuickBird image 0.6m resolution) and the 3D-image view was used in landslide identification and mapping on a GIS platform (Fig 4, 9a, c, d). Landslides attributed database was prepared for the study area (vector landslide inventory map). About 000 landslides and different erosional features were mapped. The data was verified according to the extensive field investigation. Different types of landslides were detected in satellite imagery according to special characteristics of the landslides and the erosional features. These features include erosion features, scarps~~es~~, slides, materials size, shape, tone contrast and morphological expression, and fallen materials (Fig. 9). Many potential landslide zones (rockfalls, rock sliding, circular failures, and debris channels) and erosion problems were mapped and investigated ~~on~~ using the high resolution satellite image using ArcGIS 10.2 (Fig. 5, 9). The high resolution satellite image and the high resolution 3D-image were compared with the field investigation for the same area (Fig. 9a, b). The areas affected by landslide showed high differences in their tone than the surrounding materials as well as in some instances there are fallen materials under the landslide areas (Fig. 9). Areas with landslides have typical~~ly~~ elliptical in shape. Field checking was carried out and corrections were incorporated on the image to draw the boundary lines of the landslides. These different types of landslides and erosion features along the study area are shown in Figs. 5, 9. The active portions of the landslides as observed in the field were considered as problematic areas which located above the highway and the bridge piles. All data were collected and assembled together ~~using Arc GIS 10.2~~ to create a landslide and erosion inventory map of the study area (Fig. 10). This final map shows the distribution of different types of landslides and erosion features problems in the study area including locations of debris flows, rockfalls, translational sliding, few rotational failures and erosional features along different gullies. Table (4) shows the statistical distribution of these different types of landslides according to the type of investigation and analysis. Data shows that according to the field investigation 77 landslide locations were detected and from the satellite image interpretation and 66 landslides were mapped. Some of these landslides have a direct impact on the highway and bridge section in the study area.

Fig. 9. About here

Fig. 10. About here

Table 4. About here

6 Mitigation strategies

From engineering point of view there are various types of measures that can be used to reduce the impact of landslides on the highway (Bridge section) section between tunnel 7 and tunnel 8. An outline of different mitigation methods for debris flows and landslides as potential methods were given by different authors (deWolfe, 2006; deWolfe et al., 2008; Franzi et al., 2011; Huebl and Fiebiger, 2005; Maerz et al., 2014; Wagenbrenner et al., 2006; You et al., 2012; Youssef et al., 2012, 2014b).

In the current study different mitigation and remediation techniques could be used from future landslides and erosional flows. The generation of debris flow, runoff erosion, sliding failures, and rockfalls processes acting on the entire study area were taken into account. For the current study, the slides, rockfalls, debris flows and running water cause different type of problems. The effectiveness of landslide and erosion control treatments in the study area has been evaluated. Thus the aim of mitigation is to prevent different types of landslides and running water effect (erosion problems between bride piles), which includes reducing the velocity of water flow, preventing down cutting erosion and decreasing the gradient of the gully. The mitigation methods proposed in the current study include:

1) Controlling the landslides by applying a suitable remediation/mitigation technique. Slope stabilization has to be done for the rock cuts and slopes above the bridge and highway level, this will reduce the volume of the initial material. For the unstable faces, shotcrete (the sprayed concrete process) have to be applied. Drainage ditches has to be established above the potential failures to divert the water and prevent infiltration into potential unstable areas, and benches have to be cleaned and established below the potential failures to increase the space to accommodate the falling rocks.

2) ~~for~~For the gullies with the effect of debris flows and erosion features, land management techniques have to be applied to decrease the erosional features by runoff diversion from the gullies at different levels along the benches. In the areas surrounding the bridge piles and under the culverts from up and down streams sides a layer of shotcrete need to be established in order to protect the area from scouring effect and protect the piles and culvert from any damage. In addition along the gullies grid dams need to be installed to reduce the velocity of water flow by decreasing the gradient of the gully and to stabilize slopes. This will provide barriers against runoff to reduce the erosion and resulting in a reduction for erosion potential.

7 Conclusions

In the upper portion of Tayyah valley in Asir region, Saudi Arabia, there are many active landslides and erosion features (due to runoff and debris flows along the gullies that dissect the study area) particularly along the escarpment road (highway and bridge section) between tunnels 7 and 8, which are not only threatening human lives, but also causing damages to highway and bridge foundation. Rainfall in the study area can cause different types of landslides such as debris flows along the existing gullies that will increase the erosion effect along these gullies. These debris flows and erosion effect will impact the areas under and between the bridge piles and under the culverts making undercutting features. In this study, a detailed study along the upper portion of Al-Tayyah escarpment highway between tunnel 7 and tunnel 8 was conducted to prepare landslide and erosion features inventory map. Field investigation indicated that the study area is classified into three zones, according to the RMR and the geological engineering characteristics of these zones. Zone (1) is characterized by high foliated rocks (Schistose rocks) and it is dominated by planar and rockfalls type of failures; zone (2) (fault zone area) is characterized by sheared and crashed rocks and this zone is dominated by circular type of failure; and zone (3) is characterized by moderately jointed rocks and this zone is dominated by planar and rockfalls types of failures. Debris flows and erosion features along the gullies are distributed in all zones and it is more effective and high dense in zone (2) due it its lithological and structural characteristics where most of this zone is sheared and crushed materials due to the fault. As well, different types of landslides were detected including planar sliding, circular failures, rockfalls and debris flows. Landslide and erosion features inventory map was prepared according to a coupling of the interpretation of high resolution satellite image, 3D-image view and field surveys. The results show that at least 143 landslides and erosional features were identified and mapped in the study area. These landslide and erosional features inventories have great significance for the ~~research~~ detail assessment of landslide susceptibility, distribution, and hazard assessment, as well as for the prevention and mitigation techniques. Different types of mitigation techniques have been proposed to protect, minimize, and/or prevent the impact of these landslides and runoff erosional features of the gullies on the study area.

References

Antonini, G., Ardizzone, F., Cardinali, M., Galli, M., Guzzetti, F., and Reichenbach, P.: Surface deposits and landslide inventory map of the area affected by the 1997 Umbria– Marche earthquakes. Bollettino della Societa Geologica Italiana, 121 (2), 843–853, 2002a.

Badger, T. C. and Lowell, S.: Rockfall Control Washington State. In Rockfall Prediction and Control and Landslide Case Histories, Transportation Research Record, National Research Council, Washington, 1342, 14-19, 1992.

Bajracharya, B., and Bajracharya, S. R.: Landslide mapping of the Everest region using high resolution satellite images and 3D visualization. Mountain GIS e-Conference. WWW Page http://www.mtnforum.org/sites/default/files/pub/landslide.pdf, 2008.

Bălteanu, D., Chendeş, V., Sima, M., and Enciu, P.: A country-wide spatial assessment of landslide susceptibility in Romania. Geomorphology, 124, 102–112. doi:10.1016/j.geomorph.2010.03.005, 2010.

Baum, R. L. and Godt, J. W.: Early warning of rainfall-induced shallow landslides and debris flows in the USA, Landslides, 7, 259-272. doi: 10.1007/s10346-010-0204-1, 2010.

Bieniawski, Z. T.: Engineering classification of jointed rock masses. Trans. S. Afr. Inst. Civ. Eng., v. 15, pp. 335-344, 1979.

Brabb, E. E.: The world landslide problem. Episodes, 14 (1), 52–61, 1991..

Brunsden, D.: Landslide types, mechanisms, recognition, identification. In: Morgan, C.S. (Ed.), Landslides in the South Wales Coalfield, Proceedings Symposium. The Polytechnic of Wales, pp. 19–28, , 1985..

Cardinali, M., Galli, M., Guzzetti, F., Ardizzone, F., Reichenbach, P., and Bartoccini, P.: Rainfall induced landslides in December 2004 in south-western Umbria, central Italy: types, extent, damage and risk assessment. Natural Hazards and Earth System Sciences, 6, 237–260, 2006.

Casagli, N., Fanti, R., Nocetini, M., and Righini, G.: Assessing the capabilities of VHR Satellite data for debris flow mapping in the Machu Picchu area. In: Sassa, K., Fukuoka, H., Wang, F., Wang, G. (Eds.), Landslides: Risk Analysis and Sustainable Disaster Management. Springer, pp. 61–70, 2005.

Casali, J., Lopez, J. J., and Giraldez, J. V.: Ephemeral gully erosion in southern Navarra (Spain), Catena, 36, 65-84, 1999.

Cheng, K.S., Wei, C., Chang, S.C., 2004. Locating landslides using multi-temporal satellite images. Advances in Space Research 33 (3), 96–301.

Cruden, D. M., and Varnes, D. J.: Landslide types and processes. In: Turner, A.K., Schuster, R.L. (Eds.), Landslides, Investigation and Mitigation, Special Report 247. Transportation Research Board, Washington D.C., pp. 36–75. ISSN: 0360-859X, ISBN: 030906208X, 1996.

De Blasio, F. V.: Landslides in Valles Marineris (Mars):: a possible role of basal lubrication by sub-surface ice. Planetary and Space Science 59, 1384–1392. doi:10.1016/j.pss.2011.04.015, 2011

De La Ville, N., Diaz, A. C., and Ramirez, D.: Remote sensing and GIS technologies as tools to support sustainable management of areas devastated by landslides, Environment, development and sustainability, 4, 221-229, 2002.

deWolfe, V.: An evaluation of erosion control methods after wildfire in debris-flow prone areas, M.S. thesis, Colorado School of Mines, Golden, CO. 185 PP, 2006.

deWolfe, V., Santi, P., Ey, J., and Gartner, J. Effective debris flow mitigation at Lemon Dam, LaPlata County, Colorado, Geomorphology, 96, 366-377, 2008.

Farrokhnia, A., Pirasteh, S., Pradhan, B., Pourkerman, M., and Arian, M.: A recent scenario of mass wasting and its impact on the transportation in Alborz Mountains, Iran: contribution from Geo information technology, Arab. J. Geosci., 4, 1337-1349, 2010.

Ferretti, A., Prati, C., and Rocca, F.: Non-linear subsidence rate estimation using permanent scatterers in differential SAR interferometry. IEEE Transaction on Geoscience and Remote Sensing 38, 2202–2212, 2000.

Fiorucci, F., Cardinali, M., Carlà, R., Rossi, M., Mondini, A. C., Santurri, L., Ardizzone, F., and Guzzetti, F.: Seasonal landslides mapping and estimation of landslide mobilization rates using aerial and satellite images. Geomorphology 129 (1–2), 59–70. doi:10.1016/j.geomorph.2011.01.013, 2011

Franklin, J. A. and Senior, S. A.: Rockfall Hazards – Strategies for detection, assessment, and remediation. Paper presented at: Proceedings International Symposium on Engineering Geology and The Environment; Athens, Greece, 657-663, 1997.

Franzi, L., Giordan, D., Arattano, M., Allasia, P., and Arai, M.: Preface results of the open session on ‘‘Documentation and monitoring of landslides and debris flows’’ for mathematical modelling and design of mitigation measures, held at the EGU General Assembly 2009, Nat Hazards Earth Syst. Sci., 11, 1583-1588, 2011.

Frenez, T., Roth, A., and Kaestli, A.: Debris Flow Mitigation by Means of Flexible Barriers, Pare presented at: Proceedings of the 10th Congress Interpraevent 2004; Trento, Italy, 2004.

Gagnon, H.: Remote sensing of landslide hazards on quick clays of eastern Canada. Proceeding 10th International Symposium Remote Sensing of Environment. Environmental Research Institute of Michigan, Ann Arbor, Michigan II, pp. 803–810, 1975

Gao, J., and Maroa, J.: Topographic controls on evolution of shallow landslides in pastoral Wairarapa, New Zealand, 1979–2003. Geomorphology 114 (3), 373–381. doi:10.1016/j.geomorph.2009.08.002, 2010.

Greenwood, W. R.: Geologic map of the Abha quadrangle, sheet 18 F, Kingdom of Saudi Arabia, Ministry of Petroleum and Mineral Resources, Deputy Ministry for Mineral Resources GM-75 c, scale 1:250,000, 1985.

Guzzetti, F., Cardinali, M., and Reichenbach, P.: The influence of structural setting and lithology on landslide type and pattern. Environmental and Engineering Geoscience 2 (4), 531–555, 1996

Guzzetti, F., Ardizzone, F., Cardinali, M., Galli, M., and Reichenbach, P.: Distribution of landslides in the Upper Tiber River basin, central Italy. Geomorphology 96, 105–122, 2008.

Guzzetti, F., Peruccacci, S., Rossi, M., and Stark, C. P.: The rainfall intensity duration control of shallow landslides and debris flows: an update, Landslides, 5, 3-17, 2008.

Guzzetti, F., Ardizzone, F., Cardinali, M., Galli, M., Rossi, M., and Valigi, D.: Landslide volumes and landslide mobilization rates in Umbria, central Italy. Earth and Planetary Sciences Letters 279, 222–229. doi:10.1016/j.epsl.2009.01.005, 2009.

Guzzetti, F., Mondini, A. C., Cardinali, M., Fiorucci, F., Santangelo, M., and Chang K. T.: Landslide inventory maps: New tools for an old problem. Earth-Science Reviews 112, 42–66, 2012.

Haneberg, W. C., Cole, W. F., Kasali, G.: High-resolution lidar-based landslide hazard mapping and modeling, UCSF Parnassus Campus; San Francisco, USA. Bulletin of Engineering Geology and the Environment 68, 263–276. doi:10.1007/s10064-009-0204-3, 2009.

Harp, E. L., Keefer, D. K., Sato, H. P., and Yagi, H.: Landslide inventories: the essential part of seismic landslide hazard analyses. Engineering Geology 122 (1), 9-21, 2011a.

Hoek, E., and Bray, J. W.: Rock Slope Engineering, In-stitution of Mining and Metallurgy, London, 1981.

Hoek, E.: Recent Rock Slope Stability Research at the Royal School of Mines, London," In: C.O. Brawner and V. Milligin, Eds, Geotechnical practice for stability in open pit mining, The American Institute of Mining, Met-allurgical, and Petroleum Engineers, Inc., New York, p. 27, 1982.

Hooper, A., Zebker, H., Segall, P., and Kampes, B.: A new method for measuring deformation on volcanoes and other natural terrains using InSAR persistent scatterers. Geophysical Research Letters 31, L23611. doi:10.1029/2004GL021737, , 2004.

Hooper, A., Segall, P., and Zebker, H.: Persistent scatterer interferometric synthetic aperture radar for crustal deformation analysis,with application to Volcán Alcedo, Galápagos. Journal of Geophysical Research 112, B07407. doi:10.1029/2006JB004763, 2007.

Huang, S., and Chen, B.: Integration of Landsat and terrain information for landslide study. Proceedings of 8th Thematic Conference on Geological Remote Sensing. ERIM, Denver, Colorado (USA), pp. 743–754, 1991.

Huebl, J. and Fiebiger, G.: Debris flow mitigation measures, Debris-flow Hazards and Related Phenomena, Matthias and Hung red, Springer, Berlin, 445-488, 2005.

Hungr, O., Evans, S. G., Bovis, M. J., and Hutchinson, J. N.: A review of the classification of landslides in the flow type, Environmental and Engineering Geoscience, VII, (3), 221-228, 2001.

Iverson, R. M., Reid, M. E., Logan, M., LaHusen, R. G., Godt, J. W., and Griswold, J. P.: Positive feedback and momentum growth during debris-flow entrainment of wet bed sediment, Nature Geoscience, 4, 116-121, 2011.

Johnson, A. M.: Debris flow. In: Brunsden D, Prior DB, editors. Slope Instability; New York, Wiley, P. 257-361, 1984.

Keefer, D. K.: Statistical analysis of an earthquake-induced landslide distributiondthe 1989 Loma Prieta, California event. Engineering Geology 58 (3-4), 231-249, 2000.

Lauknes, T. R., Piyush Shanker, A., Dehls, J. F., Zebker, H. A., Henderson, I. H. C., and Larsen, Y.: Detailed rockslide mapping in northern Norway with small baseline and persistent scatterer interferometric SAR time series methods. Remote Sensing of Environment 114, 2097–2109. doi:10.1016/j.rse.2010.04.015, 2010.

Lee, S., and Lee, M. J.: Detecting landslide location using KOMPSAT 1 and its application to landslide-susceptibility mapping at the Gangneung area, Korea. Advances in Space Research 38 (10), 2261–2271, 2006.

Lin, P.S., Lin, J. Y., Hung, H. C., and Yang, M. D.: Assessing debris flow hazard in a watershed in Taiwan. Engineering Geology 66, 295–313, 2002.

Maerz, N. H., Youssef, A. M., Pradhan, B., and Bulkhi, A.: Remediation and mitigation strategies for rock fall hazards along the highways of Fayfa Mountain, Jazan Region, Kingdom of Saudi, Arabia Arab J Geosci, DOI 10.1007/s12517-014-1423-x, 2014.

Marcelino, E. V., Formaggio, A. R., and Maeda, E. E.: Landslide inventory using image fusion techniques in Brazil. International Journal of Applied Earth Observation and Geoinformation 11, 181–191, 2009.

Martha, T. R., Kerle, N., Jetten, V., van Westen, C., and Vinod Kumar, K.: Characterising spectral, spatial and morphometric properties of landslides for semi-automatic detection using object-oriented methods. Geomorphology 116, 24–36, 2010.

Nichol, E. J., Shaker, A., and Wong, M. S.: Application of high-resolution stereo satellite images to detailed landslide hazard assessment. Geomorphology, 76, 68–75, 2006.

Parker, R. N., Densmore, A. L., Rosser, N. J., de Michele, M., Li, Y., Huang, R., Whadcoat, S., and Petley, D. N.: Mass wasting triggered by the 2008 Wenchuan earthquake is greater than orogenic growth. Nature Geoscience 4 (7), 449–452. doi:10.1038/ ngeo1154, 2011.

Pradhan, B., and Lee, S.: Utilization of optical remote sensing data and GIS tools for regional landslide hazard analysis using an artificial neural network model. Earth Science Frontiers, 14 (6), 143-151, 2007.

Pradhan, B., and Lee, S.: Landslide susceptibility assessment and factor effect analysis: backpropagation artificial neural networks and their comparison with frequency ratio and bivariate logistic regression modelling. Environmental Modelling & Software, 25 (6), 747-759, 2010.

Peel, M. C., Finlayson, B. L., and McMahon, T. A.: Updated world map of the Köppen Geiger climate classification, Hydrol. Earth Syst. Sci., 11, 1633-1644. ISSN 1027-5606. [http://www.hydrol-earth-syst-sci.net/11/1633/2007/hess-11-1633-2007.html, 2007.

Petley, D. N.: The global occurrence of fatal landslides in 2007, Geophysical Research Abstracts, Vol. 10, EGU General Assembly 2008. 3 pp, 2008.

Pierson, T. C. and Costa, J. E.: A rheologic classification of subaerial sediment-water flows. In: Costa JE, Wieczorek GF, editors, Debris flows/avalanches: process, recognition and mitigation, Reviews in Engineering Geology, Geol. Soc. Am., 1-12, 1987.

Plafker, G., Ericksen, G. E., and Fernández Concha, J.: Geological aspects of the May 31, 1970, Peru earthquake. Bulletin of the Seismological Society of America, 61 (3), 543-578, 1971.

Poesen, J. W. A. and Hooke, J. M.: Erosion, flooding and channel management in the Mediterranean environments of southern Europe, Prog. Phys. Geogr., 21, 157-199, 1997.

Poesen, J., Vandekerckhove, L., Nachtergaele, J., Oostwoud Wijdenes, D., Verstraeten, G., and Van Wesemael, B.: Gully erosion in dry land environments. In: Bull, L.J., Kirkby, M.J. (Eds.), Dry land Rivers: Hydrology and Geomorphology of Semi-Arid Channels. Wiley, Chichester, England, 229-262, 2002.

Poesen, J., Nachtergael, J., Verstraeten, G., and Valentin, C.: Gully erosion and Environmental change: Importance and research needs, Catena, 50, 91–133, 2003.

Pourghasemi, H. R., Mohammadi, M., and Pradhan, B.: Landslide susceptibility mapping using index of entropy and conditional probability models at Safarood Basin, Iran, Catena, 97, 71–84, http://dx.doi.org/10.1016/j.catena.2012.05.005, 2012.

Regmi, A. D., Yoshida, K., Dhital, M. R., and Devkota, K.: Effect of rock weathering, clay mineralogy, and geological structures in the formation of large landslide, a case study from Dumre Besei landslide, Lesser Himalaya Nepal, Landslides, doi: 10.1007/s10346-011-0311-7, 2013a.

Regmi, A. D., Devkota, K. C., Yoshida, K., Pradhan, B., Pourgasemi, H. R., Kumamoto, T, and Akgun, K.: Application of frequency ratio, statistical index, and weights-of evidence models and their comparison in landslide susceptibility mapping in Central Nepal Himalaya, Arab. J. Geosci, doi: 10.1007/s12517-012-0807-z, 2013b.

Regmi, A. D., Yoshida, K., Nagata, H., and Pradhan. B.: Rock toppling assessment at Mugling–Narayanghat road section: ‘A case study from Mauri Khola landslide’, Nepal, Catena, 114, 67-77, Doi.org/10.1016/j.catena.2013.10.013, 20114.

Rickenmann, D.: Empirical relationships for debris flows, Nat. Hazards, 19, 47-77, 1999.

Rimbock, A. and Strobl, T.: Rope Nets for Woody Debris Entrapmentin Torrents, Technical document of the Technische Universitat Muchen, 2002.

Rocscience, Ltd.: DPS 5.0 software for graphical and statistical analysis of orientation based geological data. Toronto, Ontario, Retrieved on 23th July, 2011 from www.rocscience.com, 1999.

Shroder, J. F. and Bishop, M. P.: Mass movement in the Himalaya: new insights and research directions, Geomorphology, 26, 13-35, 1998.

Trigila, A., Iadanza, C., and Spizzichino, D.: Quality assessment of the Italian landslide inventory using GIS processing. Landslides 7, 455–470. doi:10.1007/s10346-010-0213-0, 2010

Turner, A. K., and Schuster, R. L. (Eds.): Landslides: investigation and mitigation. National Research Council, Transportation Research Board Special Report, 247. Washington, D.C.,673 pp. 1996

Valcárcel, M., Taboada, M. T., and Dafonte, J.: Ephemeral gully erosion in northwestern Spain, Catena, 50, 199-216. 2003.

Van Den Eeckhaut, M., Poesen, J., Verstraeten, G., Vanacker, V., Moeyersons, J., Nyssen, J., van Beek, L. P. H., and Vandekerckhove, L.: Use of LIDAR-derived images for mapping old landslides under forest. Earth Surface Processes and Landforms 32, 754–769, 2007 doi:10.1002/esp. 1417.

Van Westen, C. J., Van Asch, T. W. J., and Soeters, R.: Landslide hazard and risk zonation - why is it still so difficult?, Bulletin of Engineering Geology and the Environment, 65, 167-184, 2006. doi:10.1007/s10064-005-0023-0.

van Westen, C. J., Castellanos Abella, E. A., and Sekhar, L. K.: Spatial data for landslide susceptibility, hazards and vulnerability assessment: an overview. Engineering Geology 102, 112–131, 2008.

Vargas, G. C.: Methodologie pour lestablissement de cartes de sensibilité aux mouvements de terrain fonde sur l'utilisation d'un couple stereographique SPOT XS/TM. Aplication á la region de Paz del Rio (Colombie): Proc. Ler Simposio International sobre Sensores Remotos y Sistemas de Informacion Geografica (SIG) para el estudio de Riesgos Naturales, Bogotà, Colombia, pp. 201–220, 1992

Xu C.: Preparation of earthquake-triggered landslide inventory maps using remote sensing and GIS technologies: Principles and case studies. Geoscience Frontiers xxx 1-12, 2014.

Xu, C., Dai, F. C., Xu, X. W., and Lee, Y. H.: GIS-based support vector machine modeling of earthquake-triggered landslide susceptibility in the Jianjiang River watershed, China. Geomorphology 145-146, 70-80, 2012a.

Xu, C., Xu, X. W., Dai, F. C., and Saraf, A. K.: Comparison of different models for susceptibility mapping of earthquake triggered landslides related with the 2008 Wenchuan earthquake in China. Computers & Geosciences 46, 317-329, 2012b.

Xu, C., Xu, X. W., Yao, X., Dai, F. C.: Three (nearly) complete inventories of landslides triggered by the May 12, 2008 Wenchuan Mw 7.9 earthquake of China and their spatial distribution statistical analysis. Landslides. http://dx.doi.org/10.1007/s10346-013-0404-6, 2013a.

You, Y., Liu, J. F., Pan, H. L., and Chen, X. Z.: Debris flow hazards and the optimal characteristics of the drainage canal for Zhangjia gully, Beichuan county following the 5.12 Wenchuan earthquake, Environ Earth Sci., 65, 1005-1012, 2012.

Youssef, A., M.: Landslide Susceptibility Delineation in the Ar-Rayth Area, Jizan, Kingdom of Saudi Arabia, by using analytical hierarchy process, frequency ratio, and logistic regression models. Environ earth sci. doi:10.1007/s12665-014-4008-9, 2015.

Youssef, A. M., Maerz, N. H., and Hassan A. M.: Remote sensing applications to geological problems in Egypt: case study, slope instability investigation, Sharm El-Sheikh/Ras-Nasrani Area, Southern Sinai, Landslides, 6, 353-360. doi: 10.1007/s10346-009-0158-3, 2009.

Youssef, A. M., Maerz, H. N., and Al-Otaibi, A. A.: Stability of rock slopes along Raidah escarpment road, Asir Area, Kingdom of Saudi Arabia, J. Geogr. Geol. doi:10.5539/jgg.v4n2p48, 2012.

Youssef, A. M., Pradhan, B., and Maerz, N. H.: Debris flow impact assessment caused by 14 April 2012 rainfall along the Al-Hada Highway, Kingdom of Saudi Arabia using high-resolution satellite imagery, Arab. J. Geosci., 7, 2591-2601. Doi: 10.1007/s12517-013-0935-0, 2013.

Youssef, A. M., Al-kathery, M., and Pradhan, B.: Landslide susceptibility mapping at Al-Hasher Area, Jizan (Saudi Arabia) using GIS-based frequency ratio and index of entropy models, Geosciences Journal, DOI 10.1007/s12303-014-0032-8, 2014a.

Youssef, A. M., Al-kathery, M., Pradhan, B., and Elsahly, T.: Debris flow impact assessment along the Al-Raith Road, Kingdom of Saudi Arabia, using remote sensing data and field investigations, Geomatics, Natural Hazards and Risk, doi:10.1080/19475705.2014.933130, 2014b.

Youssef, A. M., Pradhan. B., Jebur, M. N, El-Harbi., H. M.: Landslide susceptibility mapping using ensemble bivariate and multivariate statistical models in Fayfa area, Saudi Arabia. Environ Earth Sci. doi:10.1007/s12665-014-3661-3, 2014c.

Wagenbrenner, J., Macdonald, L., and Rough, D.: Effectiveness of three post-fire rehabilitation treatments in the Colorado Front Range.~~,~~ Hydrological Processes, 20, 2989-3006, 2006.

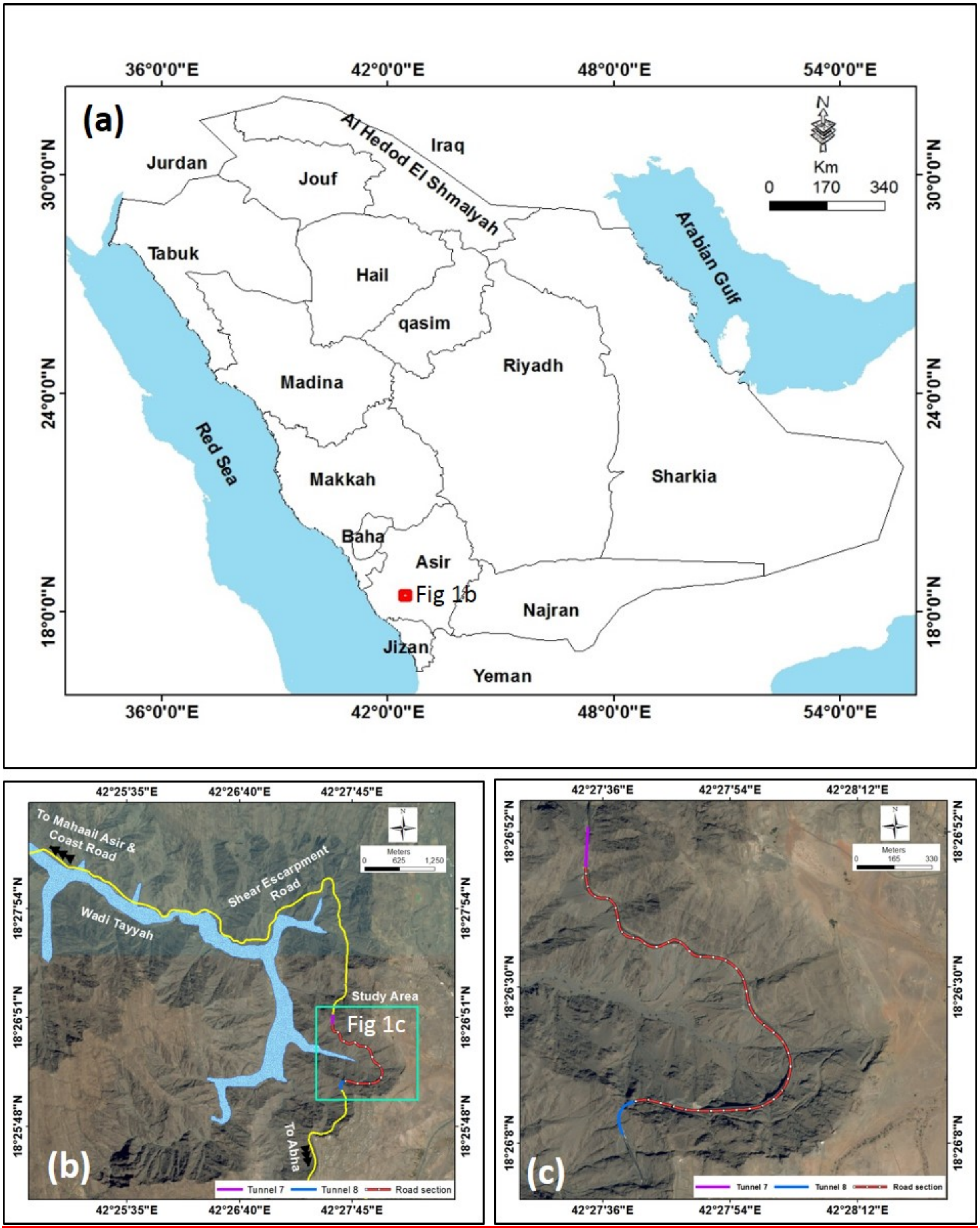
(a)
36°0'0"E
42°0'0"E
48°0'0"E
54°0'0"E
30°0'0"N
24°0'0"N
18°0'0"N
N
Km
0 170 340
Al Hedod El Shmalyah
Iraq
Jurdan
Jouf
Tabuk
Hail
qasim
Arabian Gulf
Madina
Riyadh
Red Sea
Makkah
Sharkia
Baha
Asir
Fig 1b
Najran
Jizan
Yeman
(b)
42°25'35"E
42°26'40"E
42°27'45"E
18°27'54"N
18°26'51"N
18°25'48"N
To Mahaail Asir & Coast Road
Shear Escarpment Road
Wadi Tayyah
Meters
0 625 1,250
Study Area
Fig 1c
To Abha
Tunnel 7
Tunnel 8
Road section
(c)
42°27'36"E
42°27'54"E
42°28'12"E
18°26'52"N
18°26'30"N
18°26'8"N
Meters
0 165 330
Tunnel 7
Tunnel 8
Road section

Fig. 1. a) Location of the study area in the KSA map. B) Upper portion of Tayyah Valley including the study area. C) Study area in a close up view.

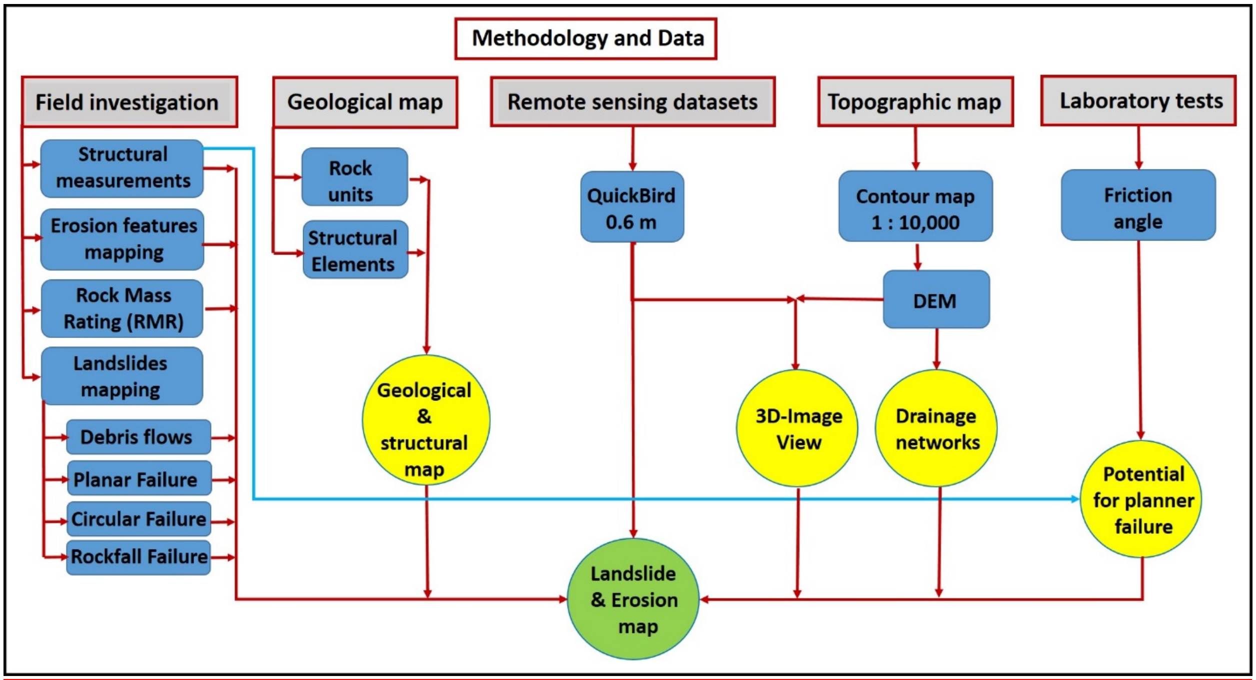

Fig. 2. Flow chart showing data used and methodology in the study area.

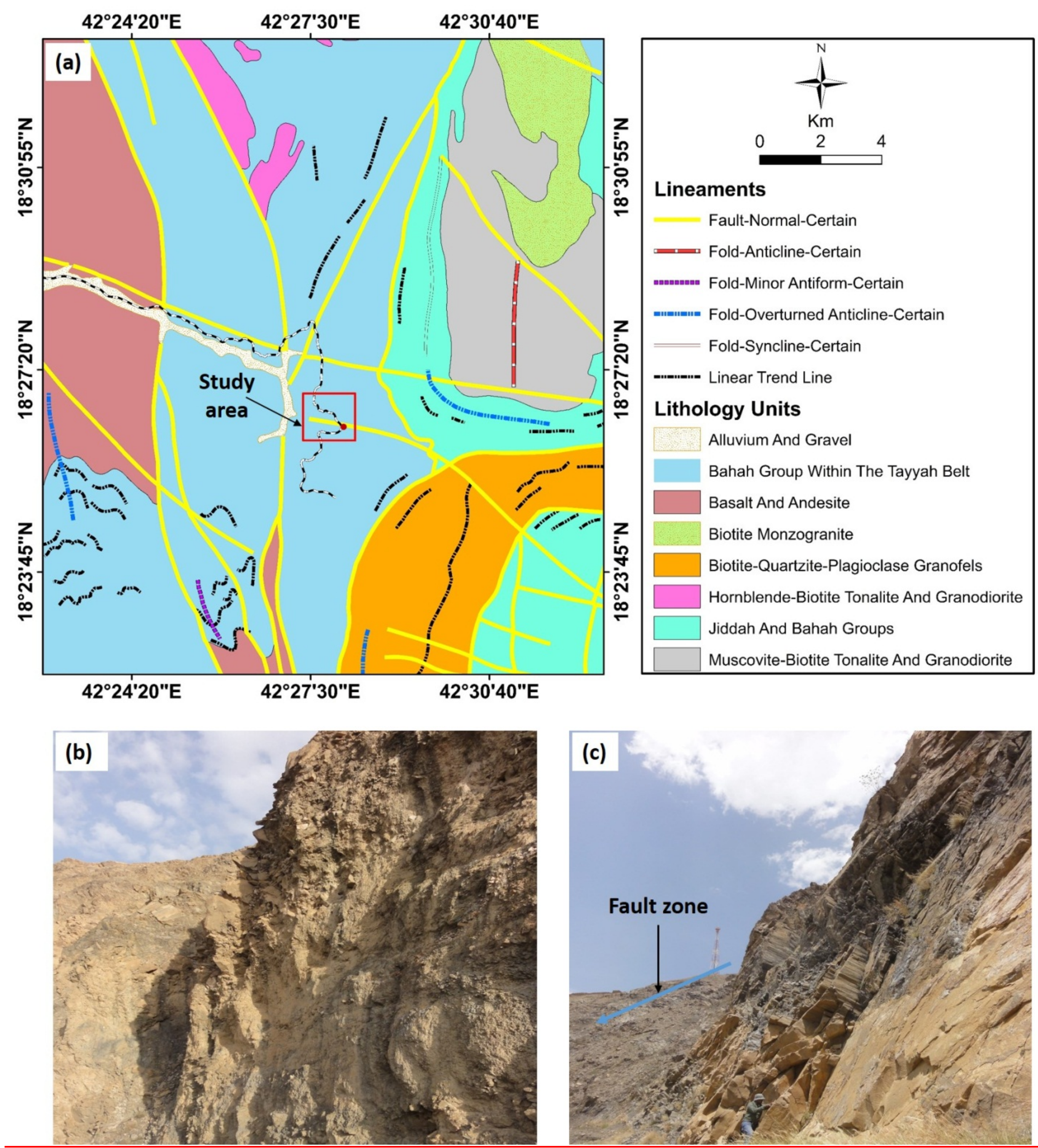

Fig. 3. a) Geological map of the study area and its surroundings at the upper portion of the Tayyah Valley, b) rocks are highly crashed along the fault zone, and c) rocks close to fault zone are highly sheared and jointed.

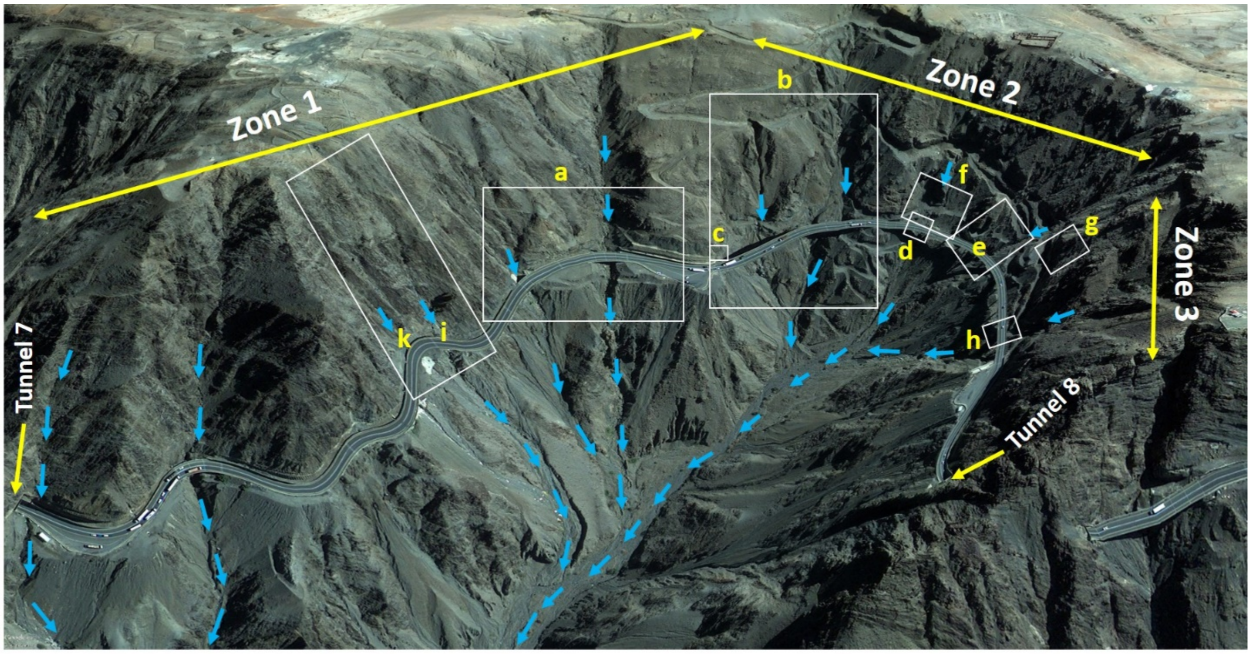

Fig. 4. 3D image view showing the potential gullies causing debris movements and erosions under and between the bridge piles as well as the areas for different types of landslides. 3 D image was prepared using QuickBird imagery. Note, the study area between tunnels 7 and 8 shows three zones and different landslides locations can be easily recognized, letters a to k are pictures in figure 5.

Fig. 5. Field photographs showing different types of landslides and erosional features along the highway and bridge section of the study area. a) sliding and erosional features due to running water along gullies, b) Sliding blocks along sliding plane (there are big blocks close to the bridge pile), c) large planar sliding, d) Potentially circular failure area where some circulare failure

happened and many curved tension cracks appeared, e) circular failure very close to the bride, f&g) Examples of curved tension cracked. h&i) Potentially rockfall failure area where some overhanging blocks appeared, j) debris channels along them erosional features and big boulders appear, k) debris materials of different sizes range from sand size up to big boulders 0.5 m in diameter, l) deep erosion and remove the materials surround one bridge pile, m) running water remove materials under the culvert make them under risk.

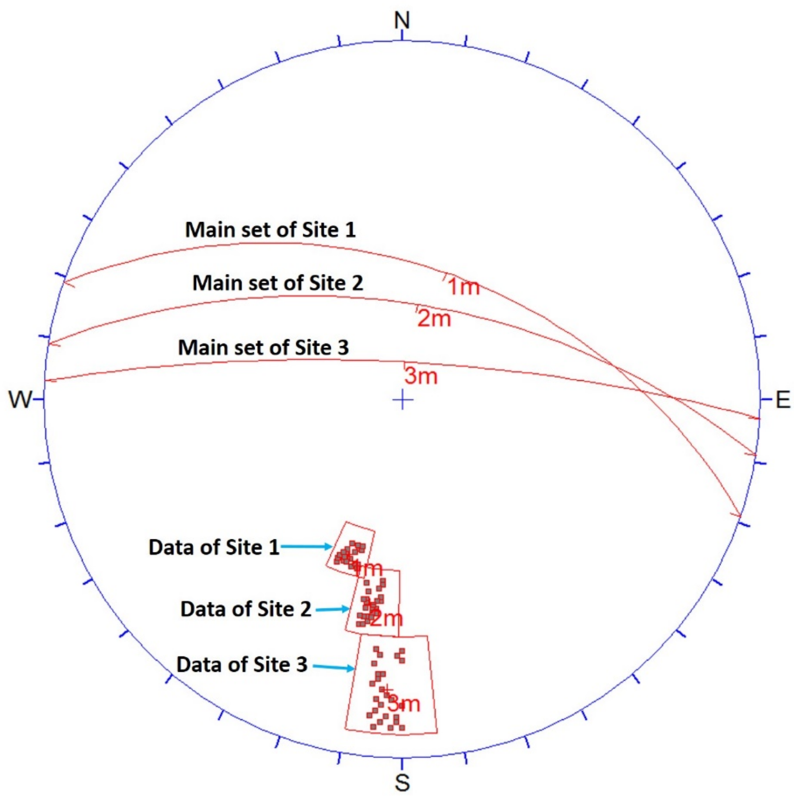

Fig. 6. Pole Plots for the data collected from the three sites.

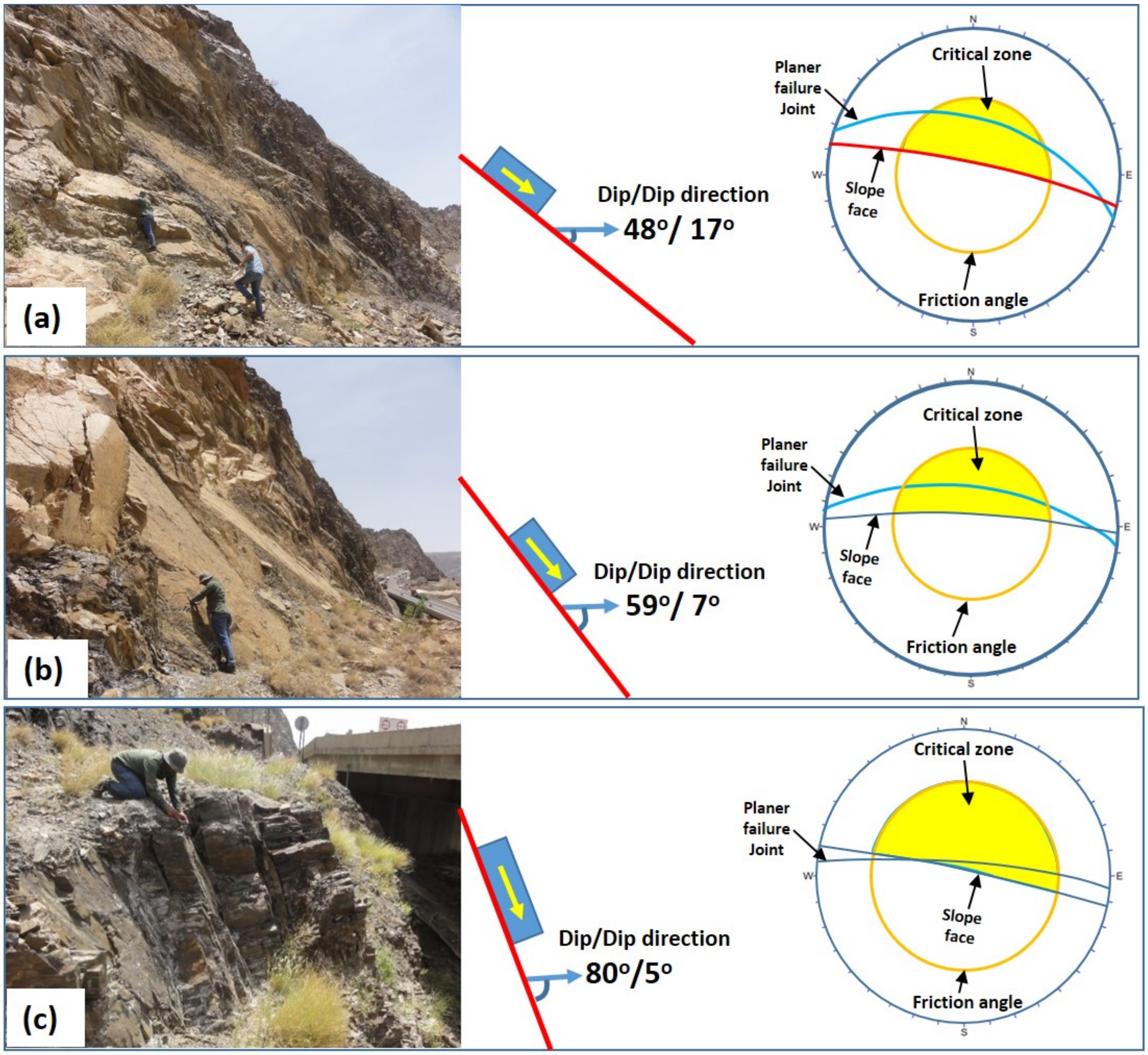

Fig. 7. The analysis used in the study for planar failures along the road section of the study area: (a, b, c) Field photographs at the three locations 1, 2, 3 respectively showing the planar joints dips toward the road section, simple sketch showing the dip/dip direction average values of plane that responsible of plannar failure for each site, and Markland Test circles showing the main set, friction angle, and rock cut face for each location plotted in Dips 5 program (note that there is potential planar failures as the plot vector of planes are located in the critical zone).

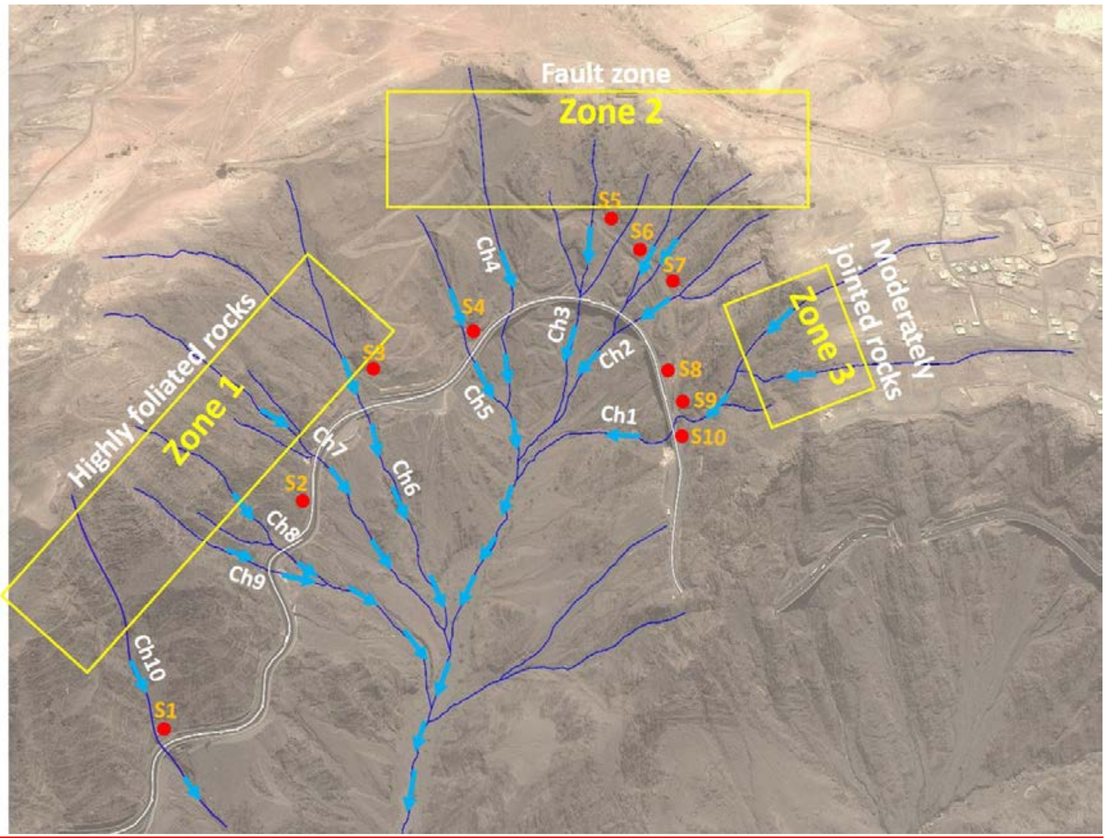

Fig. 8. Different gullies were mapped in the study area as well as the stations for RMR calculation is shown as red color dots.

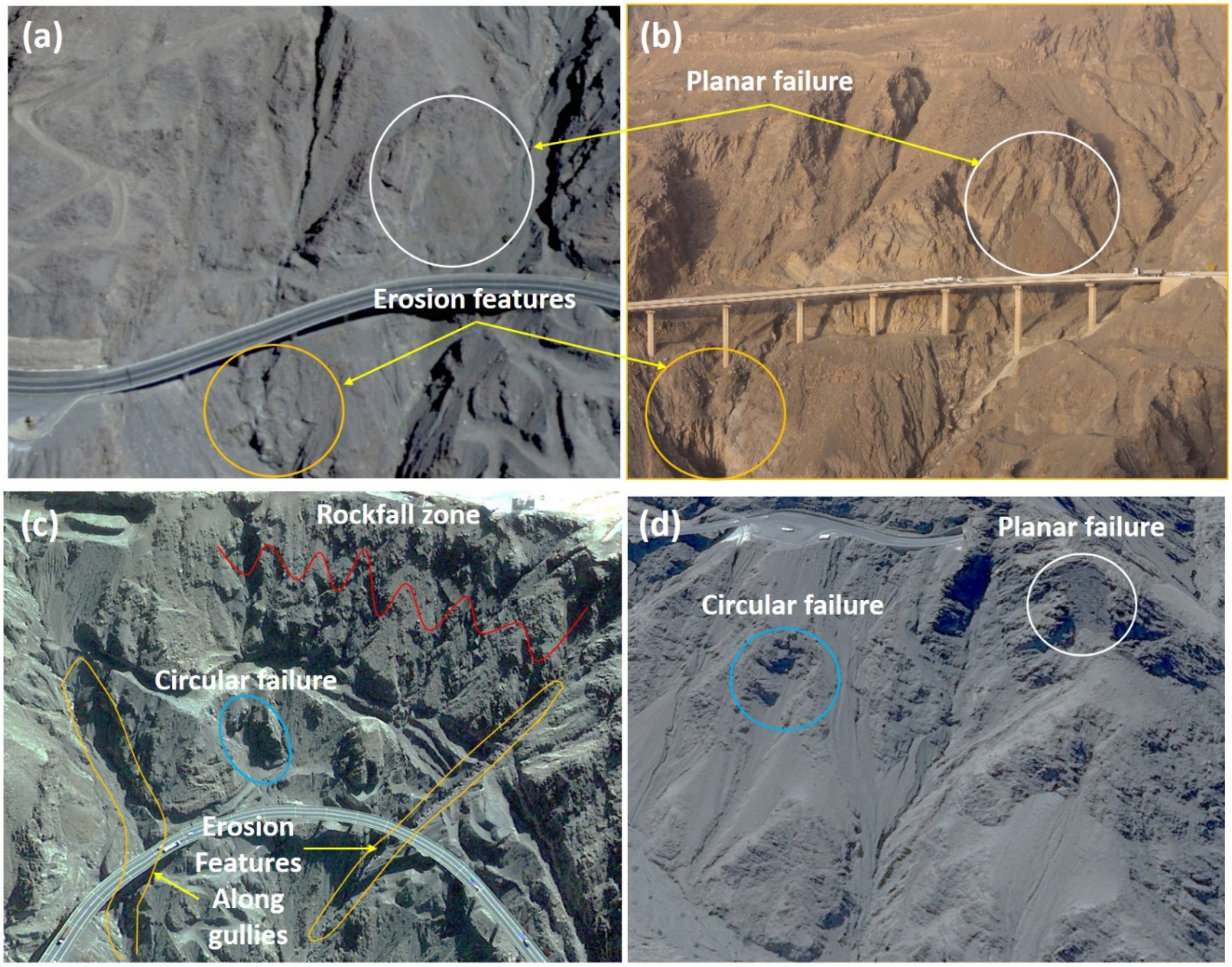

Fig. 9. a) Different landslides features can be detected using high resolution satellite image; b) same landslides features appeared in field photograph in the same area; c&d) planar, circular, rockfall zone and erosion features as they appear in high resolution satellite image (3D images)

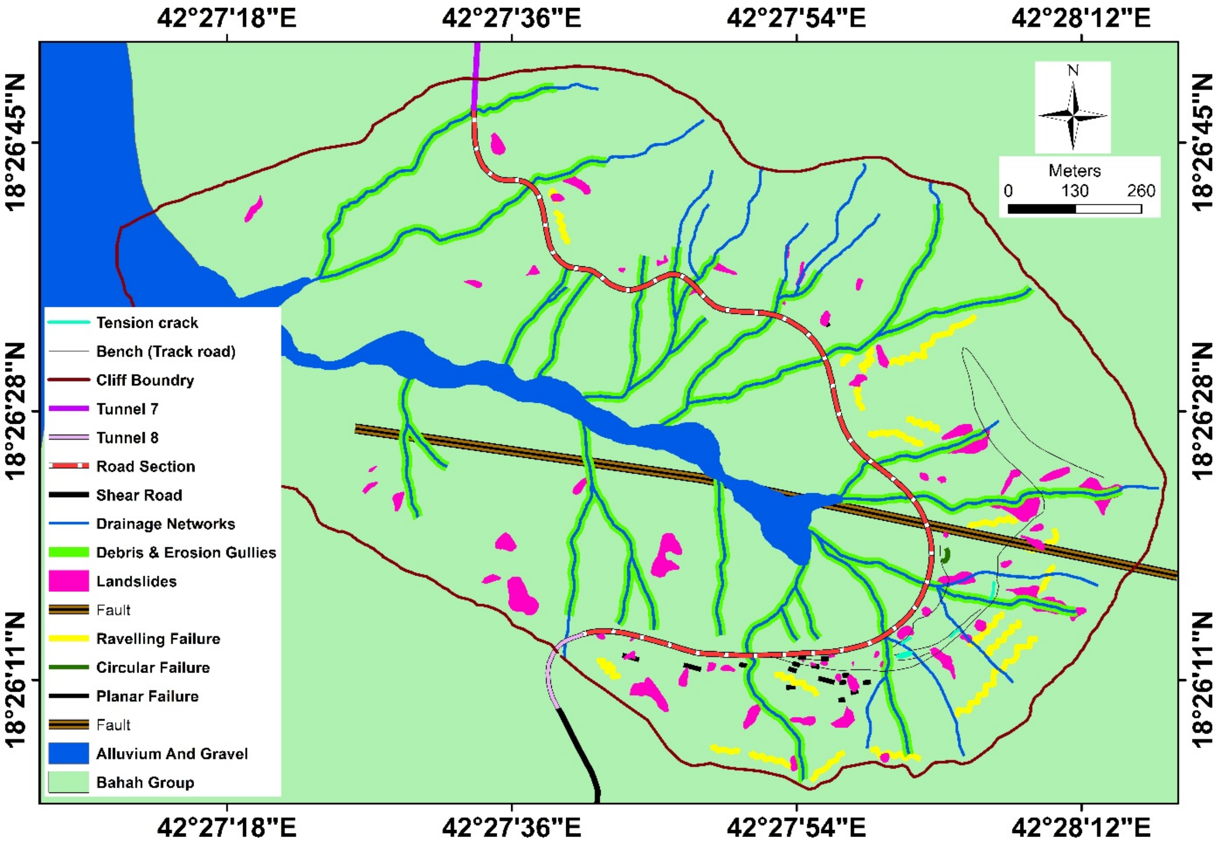

Fig. 10. Inventory map of the study area showing special distribution of different types of landslides and the erosional features (potential areas for rockfalls, planar failures, debris channels, circular failures, tension cracks and erosional features along the gullies that dissect the study area) due to visual inspection and field work.

Table 1. RMR values for different stations along the study area

Zone #	Station #	UCS MPa	RQD	Spacing of discontinuities	Condition of discontinuities	Water condition	RMR basic	Rock Class
Z1	1	1-5	<25	<60 mm	Soft gouge >5 mm thick Or Separation > 5 mm Continuous	Damp	19	Very poor rocks
	2	3-25	25- 50	60-200 m	Slickensided surfaces Or Gouge < 5 mm thick Or Separation 1-5mm	Wet	35	Poor rocks
	3	3-25	<25	<60 mm	Slickensided surfaces Or Gouge < 5 mm thick Or Separation 1-5 mm	Damp	30	Poor rocks
Z 2	4	1-5	<25	<60 mm	Soft gouge >5 mm thick Or Separation > 5 mm Continuous	Damp	19	Very poor rocks
	5	1-5	<25	<60 mm	Soft gouge >5 mm thick Or Separation > 5 mm Continuous	Wet	16	Very poor rocks
	6	1-5	<25	<60 mm	Soft gouge >5 mm thick Or Separation > 5 mm Continuous	Wet	16	Very poor rocks
	7	1-5	<25	<60 mm	Soft gouge >5 mm thick Or Separation > 5 mm Continuous	Damp	19	Very poor rocks
Z3	8	50-100	50-75	0.6-2 m	Slightly rough surfaces Separation <1 mm. Highly weathered walls	Damp	65	Good
	9	100-250	50-75	0.6-2 m	Slightly rough surfaces Separation <1 mm. Highly weathered walls	Damp	70	Good
	10	100-250	75-90	<60 mm	Slightly rough surfaces Separation <1 mm. Highly weathered walls	Damp	74	Good

Table 2. Shows different characteristics of each site

Site Number	Main Joints		Rock Cut face		Friction angle (Ø) due shear test
	Dip angle	Dip direction	Dip angle	Dip direction	
1	48^{o}	17^{o}	80^{o}	12^{o}	35
2	59^{o}	7^{o}	80^{o}	2^{o}	40
3	80^{o}	5^{o}	85^{o}	13^{o}	30

Table 3. General characteristics of the gullies and different rock zones

	Ch1	Ch2	Ch3	Ch4	Ch5	Ch6	Ch7	Ch8	Ch9	Ch10
Maximum elevation (m)	2163	2153	2145	2139	2136	2035	2127	2149	2113	2111
Minimum elevation (m)	1920	1964	1925	1835	1844	1843	1707	1793	1842	1877
Elevation difference (M)	243	189	220	304	292	192	420	356	271	234
Length (m)	826	526	319	783	588	360	587	831	598	538
Tan (θ^{o})	0.294	0.359	0.690	0.388	0.497	0.533	0.716	0.428	0.453	0.435
Slope Degree (θ^{o})	13.2^{o}	16.2^{o}	31.0^{o}	17.5^{o}	22.4^{o}	24.0^{o}	32.2^{o}	19.3^{o}	20.4^{o}	19.6^{o}
Width (m)	15	11	9	8	7	10	8	8	6	8
Depth of erosion (m)	Up to 2 meters	Up to 5 meters				Up to 3 meters				
Zone Name	Moderate jointed rocks	Fault zone				High foliated rocks				
Main characteristics	Planar failures and rockfalls	Circular failures and debris flows				Planar failure				

Table 4. Landslide types and numbers according to the used method

Study Type	Landslide Type	Number
Satellite image and 3D-image view Interpretation	Landslides (planar, circular, rockfalls, debris flows)	66
Field investigation	Planar	17
	Circular	11
	Rockfalls	20
	Debris and erosion features along the gullies	29
Total Number of landslides and erosion features		143